

Fuzzy Based Image Processing for Malaria Screening Using Deep Learning Approach

Dr.Lakshma Reddy B

Department of Computer Science Engineering,
Rajarajeswari College of Engineering, Bengaluru, India
Prof.reddy99@gmail.com

Gokul A

Department of Computer Science Engineering,
Paavai College of Engineering, Namakkal, India
gokuldominator@gmail.com

Manikandan S

Department of Computer Science Engineering,
Kongunadu College of Engineering and Technology, Namakkal, India
mail2manicse@gmail.com

Stephy Christina J

Department of Computer Science Engineering,
DMI Engineering College, Kanyakumari, India
stephy@dmiengg.edu.in



Publication History:

Manuscript Reference No: IJIRIS/RS/Vol.11/Issue04/JNIS10080

Research Article | Open Access | Double-Blind Peer-Reviewed | Article ID: IJIRIS/RS/Vol.11/Issue04/JNIS10080 Received: 02, May 2025 Revised: 12, May 2025 Accepted: 15, May 2025 Published Online: 12, June 25, Volume 2025

Article ID JNIS10080 <https://www.ijiris.com/volumes/Vol11/iss-04/01JNIS10080.pdf>

Article Citation: Dr.Lakshma,Gokul,Manikandan,Stephy(2025).Fuzzy Based Image Processing for Malaria Screening Using Deep Learning Approach. IJIRAE.: International Journal of Innovative Research in Information Security, Volume 11,Issue 04, Pages 276-283 doi:> <https://doi.org/10.26562/ijiris.2025.v1104.01>

BibTex key: Dr.Lakshma@2025Fuzzy



Copyright: ©2025 This is an open access article distributed under the terms of the Creative Commons Attribution License; which Permits unrestricted use, distribution, and reproduction in any medium, provided the original author and source are credited.

Abstract: Malaria, an infectious disease transmitted by mosquitoes, is attributed to the Plasmodium genus. The conventional method of diagnosis involves the meticulous examination of stained blood samples through a microscope. This process, while effective, is labor intensive and time-consuming. However, the integration of machine learning techniques offers a promising enhancement for analyzing microscopic images of blood smears to detect parasites. This paper reviews the diverse methodologies that have been previously utilized, with a particular emphasis on the various imaging strategies employed. A thorough summary is presented, encompassing research conducted on both thin and thick blood smear images. Additionally, the paper highlights emerging advancements in deep learning and modern mobile technologies as potential future assets for malaria diagnosis. Recent progress in machine learning techniques for the detection and identification of malaria in images is also examined, with a focus on the challenges related to image processing. Furthermore, a detailed comparison of different machine learning approaches is provided to offer a comprehensive perspective. The application of these sophisticated machine learning and deep learning techniques has the potential to transform the landscape of malaria detection and control.

Keywords: Deep Learning; Malaria; Object detection; Plasmodium falciparum; Thick smear microscopic

INTRODUCTION

Malaria is one of the most deadly illnesses and the motive of excessive mortality fee in the world, which is transmitted from contaminated to wholesome people via the bites of lady Anopheles mosquitoes. It is precipitated by way of a unicellular parasite recognised as plasmodium. Once the parasite enters the human physique it grows inner the liver and is launched to the bloodstream to infect pink bloodcells (RBCs). Plasmodium parasite has 5 species including, plasmodium falciparum (P. falciparum), plasmodium vivax (P. vivax), plasmodium ovale (P. ovale), plasmodium Knowlesi (P. knowlesi), and plasmodium malariae (P. malariae); the place P. falciparum and P. vivax are the most pathogenic and infect majority of the world population. According to information posted by using World Health Organization (WHO) malaria record 2020 an estimated 241 million malaria instances had been stated in 2020, amongst which 95% of the instances are in WHO African area with solely the ultimate 5% outdoor African region.

Globally, there had been 627,000 malaria deaths in 2020 amongst which 96% of the instances passed off in 29 countries, and six nations – Nigeria (27%), the Democratic Republic of Congo (12%), Uganda (5%), Mozambique (4%), Angola (3.4%) and Burkina Faso (3.4%) – accounted for about 55% of all instances globally [1]. There are a number of techniques for malaria analysis along with medical diagnosis, microscopic diagnosis, speedy diagnostic take a look at kits (RDTs) and polymerise chain response (PCR). Clinical prognosis is primarily based on more than a few signs of malaria such as the records of fever and it has low specificity which leads to full-size overuse of antimalarial capsules [2].

PCR is the most touchy approach however it is steeply-priced and complex, whereas RDTs are exceptionally touchy and are unable to quantify parasite density [3]. Parasitological affirmation through microscopy the usage of thin/thick blood movie stays the golden well-known for malaria diagnosis; however it is a cumbersome approach [4]. In the tactics of guide microscopy diagnosis, a skinny or thick blood smear is organized with the aid of spreading a drop of blood on a glass slide which is dried and stained earlier than being visually examined via microscopist identification. A thick smear has a giant quantity of blood and a massive wide variety of parasites per blood volume. It is typically used for finding out whether or not the patient's blood consists of malariaparasites or not. The accuracy of guide microscopic examination is severely affected by means of excessive intra/inter-observer variability which is supplemented via a massive quantity of instances recognized per day in malaria-endemic areas with low aid settings [5]. Besides, visible examination the usage of guide microscopy is tedious and time-consuming [6]. The scarcity of skilled professionals and lack of a rigorous gadget to assist understanding talent gaps at malaria endemic areas leads to mistaken prognosis effects which make a contribution to inappropriate cure [7], [8]. The challenges in the guide microscopy analysis manner encourage the lookup neighbourhood to enhance automatic computer-aided diagnostic (CAD) structures to enhance malaria prognosis accuracy and minimize the medical challenges due to human error via empowering microscopists' diagnostic choices for final higher affected person treatment.

Most current research mix regular picture processing strategies with classical desktop studying algorithms to improve computerized malaria analysis systems. Traditional picture processing processes such as adaptive threshold methods or different morphological operations have been used to section the parasite candidates from the heritage of both thick or skinny smear microscopic snap shots [9], [10],[11],[8]. However, such picture processing tactics are very touchy to versions in photo fantastic due to the fact the segmentation methods are decided empirically. On the other hand, traditional desktop mastering fashions the usage of handcrafted aspects from segmented malaria parasite place of pastime (ROI) are used for classifying malaria-infected and uninfected cells [11], [12],[13]. However, classical desktop gaining knowledge of algorithms which are primarily based on hand-engineered facets battle to generalize when their enter records area version increases. Recently, the development of deep getting to know algorithms has celebrated a lot of achievements in its software in a vary of clinical imaging duties such as scientific photograph segmentation and reconstruction [14], [15], classification duties [16],[17], and object detection [18]. Furthermore, latest research exhibit deep learning-based algorithms outperformed traditional photo processing and computing device studying strategies for detection and identification of malaria parasites the use of microscopic snap shots of skinny and thick blood smear.

Another learn about by using [19] proposed a multi pipeline method via making use of Mask-RCNN as pre-candidate *P. falciparum* and *P. vivax* species detector accompanied through classifier head to filter out false positives. They consider their detection device the use of image-level and patient-level through the usage of experimentally described threshold scores. They finished an accuracy of 90.8% on photograph degree and 97.6 accuracy on patient-level evaluation. They have used a comparable dataset to ours for *P. faciparum* detection however they did no longer consider their device at the patch level. Another find out about [20] proposed a twin deep mastering framework for RBC segmentation the usage of skinny smear images. They have used U-Net as a pre-candidate RBC cluster segmentation and utilized Faster-RCNN for the last detection of RBCs. However, they did no longer classify between malaria-infected and uninfected RBCs.

A mobile-based *P. falciparum* and white blood cell(WBC) localization the usage of pre-trained deep getting to know fashions are proposed by means of [28]. In this learn about they organized a new dataset of 903 fields stained thick blood smear microscopic pictures to instruct and consider their proposed models. Another learn about by way of [37] proposes an his learn about pursuits to enhance detection overall performance and consider the effectiveness of SOTA deep learningbased object detection fashions for *P. falciparum* detection from thick smear microscopic photos by way of fixing the aforementioned challenges described in area 1.1. To this goal, a tile-based photograph processing used to be proposed to amplify small object detection functionality of SOTA object detection algorithms for working on high-resolution thick smear microscopic photographs than their community enter decision allows. The generic overview of the proposed scheme is illustrated in Figure 1. In the proposed strategy the HR picture used to be divided into overlapping small pictures known as tiles so that every can then be fed to SOTA object detection networks barring degrading the authentic photograph resolution. During mannequin coaching tiles with their corresponding floor reality annotation mapped therefore have been used as an enter and tiles which did not have ground reality annotation had been excluded. Note that some objects may additionally be reduce at tile boundaries and the ratio of areas between partly segmented components and the full object was once taken to preserve or discard the annotation throughout mannequin training. Dividing HR snap shots into tiles enabled to enlarge the relative vicinity of small objects for the detection community enter resolution.

Datasets

To affirm the effectiveness of the proposed strategy in this work experiments had been run by using the usage of two sorts of datasets. The first one, which is referred to as mannequin improvement dataset, is used for training, validation, and trying out the proposed SOTA detection fashions and eventually to choose the satisfactory mannequin thinking about its detection accuracy and computation speed. This dataset consists of high-resolution thick smear microscopic pix contaminated with *P. falciparum* which is obtained from preceding researchers [7]. It is accrued from one hundred fifty sufferers at Chittagong Medical College Hospital, Bangladesh, and manually annotated via skilled experts. The dataset incorporates an common variety of 12 pictures per affected person and forty seven parasites per image.

The photographs are in RGB coloration and have a excessive decision of 4032 x 3024 pixels. Sample pix from the improvement dataset with their corresponding annotations

Table 1: Dataset Description

Training	Validation	Testing	Total	
Model Development Dataset				
Number of patients	90	30	40	160
Number of images	1,150	270	384	1,804
Number of parasites	48,530	11,274	23,783	83,587
External Dataset 1				
Number of images	985	109	112	1,206
Number of parasites	6,314	674	739	7,727
External Dataset 2				
Number of images	670	199	110	979
Number of parasites	7,780	490	1,078	9,348
External Dataset 3				
Number of images	-	-	-	1,141

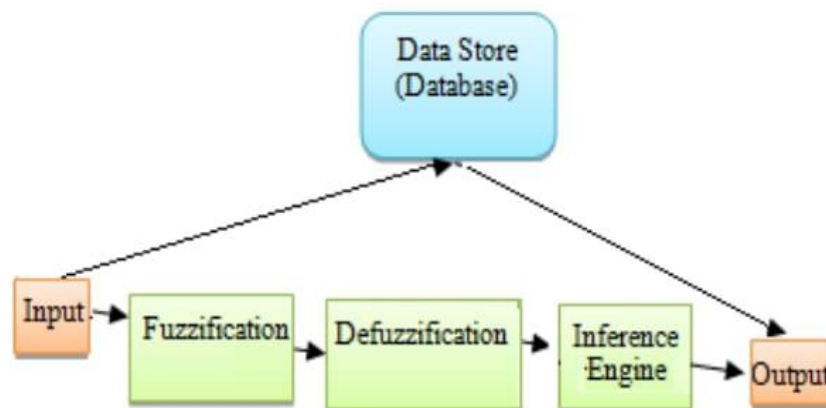


Figure1: Data flow diagram

3.2 Proposed Detection Networks The proposed P. falciparum detection algorithms had been primarily based on the YOLOV4 object detection mannequin [45] which is chosen thinking about its excessive detection overall performance and inference velocity for downstream object detection duties compared to different single-stage and two-stage detectors [45]. In this study, three distinct YOLOV4 based totally object detection fashions have been evaluated to discover the pleasant mannequin with an most beneficial trade-off between detection overall performance and inference speed. The first detection network, which is known as YOLOV4-MOD, is primarily based on preceding work [39] which is modified to enhance small object detection overall performance of the unique YOLOV4 mannequin with minimal computation cost. This mannequin has a massive variety of trainable parameters and extra convolution layers. The 2nd two detection networks are based totally on light-weight variations of YOLOV4 recognized as tiny YOLOV4 models, which are designed for increased inference pace with compromise on their detection accuracy. Among these light-weight models, the first model, which is referred to as YOLOV4-tiny, has two detection heads while the 2d detection model, which is known as YOLOV4-tiny-3l, has three detection heads.

The addition of greater detection heads on YOLO-based fashions enabled higher detection overall performance for small objects [39]. These two light-weight networks have a small variety of trainable parameters and fewer convolution and max-pooling layers in contrast to the massive dimension model.

3.3 Evaluation Metrics

In this study, two extensively used contrast metrics for object detection tasks, particularly common precision (AP) and recall (R), had been used to consider overall performance of the proposed models. The common precision is primarily based on the location underneath interpolated Precision-Recall Curve (PRC), the place precision is calculated as the ratio of the wide variety of real nice detections to all detected objects. The recall measures the fraction of detections that are real positive. The formulation for the comparison metrics are given below.

$$\text{where } \text{pinterp}(r) = \max_{p \geq r} p$$

where True Positive (TP) shows the quantity of successfully detected objects, False Positive (FP) shows the range of incorrectly estimated suspicious objects, and False Negative (FN) suggests the wide variety of undetected objects. pinterp represents the interpolated precision (p) over a given recall (r) values in an ascending order from zero to 1.0 into eleven factors — 0, 0.1, 0.2, ..., 0.9 and 1.0.

In this study, various experimental settings have been accompanied to increase and consider the effectiveness of the proposed tile-based thick smear microscopic photo processing strategy for malaria parasite screening. First, the three proposed YOLOV4 based totally detection fashions described in part 3.2 had been skilled the use of tiles with specific tile sizes generated from the mannequin improvement dataset described in part 3.1. Afterward, the pleasant mannequin is chosen thinking about its trade-off between computation velocity and detection overall performance on the mannequin improvement check data. The dataset is divided into training, validation, and checking out at affected person degree the place ninety six sufferers have been used for training, 24 sufferers for validation, and 30 sufferers for testing. In this experimental setting, most useful community hyperparameters of the detection fashions have been additionally chosen through the use of the mannequin improvement validation dataset.

After determination of the fantastic mannequin amongst the three proposed detection models, its *P. falciparum* detection overall performance was once examined on the first and 2nd exterior datasets described in part 3.1. When the chosen mannequin used to be evaluated the usage of the first exterior dataset tile-based processing was once no longer utilized considering decision of the dataset is now not excessive in contrast to the proposed detection network's enter resolution. The 2nd exterior dataset consists of high-resolution thick smear microscopic pictures and the tile-based strategy used to be utilized when it used to be evaluated the usage of this dataset. Furthermore, two experimental setups have been observed in the course of contrast of the chosen mannequin the use of these two exterior datasets. In the first experimental setting, the chosen mannequin was once evaluated via using the total dataset as check data. In the 2d experimental setting, the datasets had been partitioned into training, validation, and take a look at as proven in Table 1 and mixed with the mannequin improvement dataset to fine-tune the chosen model. In addition, the chosen mannequin was once evaluated on 1141 uninfected pictures accrued from 50 uninfected sufferers [19] which have no longer been used at some point of mannequin training. This dataset is a high-resolution thick smear microscopic photograph and has a decision of 4032 x 3024 pixels. Thus, the proposed tile-based method was once utilized to look into overall performance of the chosen mannequin on figuring out uninfected images.

Baseline Method: The proposed tile-based strategy used to be compared with a baseline technique in which a full high-resolution photograph is downsampled to the proposed SOTA detection network's enter decision both in the course of mannequin education and inference. This approach provides quick coaching and inference velocity however it leads to exact facts loss determined in the unique highresolution picture which resulted in huge detection overall performance degradation.

Proposed Detection Network Training and Hyper-parameter Optimization

During proposed mannequin training, hyperparameter optimization, and choice of first-class mannequin a publicly reachable high-resolution thick smear microscopic photo dataset amassed from [7] was once used. Different tile sizes relative to the detection network's enter decision had been utilized to stop loss of distinctive records in HR pictures and to preserve the computation value most effective as well. To overcome the trouble of a restrained dataset in all experimental settings pre-trained fashions the usage of MS COCO dataset [23] had been leveraged and fine-tuning used to be utilized through the use of the goal dataset. In the coaching process, default configurations in unique variations of the proposed YOLOV4 primarily based fashions have been used until specified.

Anchor container sizes had been modified primarily based on the community enter decision and floor fact bounding container records of the unique dataset used for training. A batch dimension of two for giant measurement YOLOV4 primarily based mannequin (YOLOV4-MOD) and a batch measurement of eight for light-weight fashions (YOLOV4-tiny and YOLOV4-tiny-3l) was once used. All the fashions have been skilled for 4000 iterations the use of the default settings for information augmentation, optimizer, and loss functions. The preliminary studying fee was once 0.001 for massive measurement mannequin and 0.00261 for light-weight fashions and diminished with the aid of a element of 10 at 80% and 90% of the coaching iteration.

The detection community enter sizes have been set as 416 x 416 and 512 x 512 for massive dimension mannequin due to computational constraint and 416 x 416, 512 x 512 and 608 x 608 for light-weight models. All the experiments had been carried out through the use of Google Colaboratory with NVIDIA TESLA K80 processor and 12 GB of RAM.

RESULTS

In Tables 2 and three element experimental effects are illustrated for the unique experimental settings described. The experimental consequences show the outcomes of quite a number strategies used in this study, consisting of one of kind detection networks proposed, variant in community enter resolution, and tile measurement version each for the duration of coaching and inference stage. By the usage of the mannequin improvement take a look at data, which consists of 30 sufferers and 374 images, amongst the proposed three detection models, YOLOV4-tiny with 512 x 512 enter decision and tile dimension of 608 x 608 each at instruct and inference time performs nicely with a most recall of 95.3% and most common precision of 87.1%. In a comparable take a look at set data, YOLOV4-tiny-3l with 608 x 608 enter decision and tile dimension of 608 x 608 each at educate and inference time accomplished a most recall.

Table 2: Comparisons of detection performance and inference speed for YOLOV4-MOD by using the proposed and baseline approach on model development test set data. Bold values indicate the best-performing model.


Model	Input Res.	Tile size		AP(%)	R (%)	sec 	
		train	Inference				
YOLOV4-MOD@416	4032 x 3024	1088 x 1088	1088 x 1088	56	60	1	
YOLOV4-MOD@608	4032 x 3024	1088 x 1088	1088 x 1088	77.9	83.4	8	
YOLOV4-MOD@416	4032 x 3024	1088 x 1088	416 x 416	67	73	1	
YOLOV4-MOD@512	4032 x 3024	608 x 608	1088 x 1088	54.3	60.8	1	
YOLOV4-MOD@512	4032 x 3024	1088 x 1088	832 x 832	82.5	92.6	5	
YOLOV4-MOD@512	4032 x 3024	832 x 832	608 x 608	81.4	88.1	1.6	
YOLOV4-MOD@416	4032 x 3024	1088 x 1088	416 x 416	65	75.9	1	
with outtiling							
YoloV4-MOD@512	4032 x 3024	-	-	79.78	80	0.25	
YoloV4-MOD@416	4032 x 3024	-	-	72.8	76	0.2	

Table 3: Comparisons of detection performance and inference speed for YOLOV4-tiny by using the proposed and baseline approach on model development test set data.

Model	Input Res.	Tile size		AP (%)	R (%)	sec/img
		Train	Inference			
YOLOV4-tiny@416	4032 x 3024	1088 x 1088	1088 x 1088	56	60	1
YOLOV4-tiny@512	4032 x 3024	1088 x 1088	832 x 832	67	73	1
YOLOV4-tiny@416	4032 x 3024	1088 x 1088	608 x 608	78	86	1.4
YOLOV4-tiny@512	4032 x 3024	1088 x 1088	416 x 416	65	75.8	1.4
YOLOV4-tiny@416	4032 x 3024	1088 x 1088	1088 x 1088	70	75.9	1
YOLOV4-tiny@512	4032 x 3024	1088 x 1088	832 x 832	80.4	86.1	1.2
YOLOV4-tiny@608	4032 x 3024	1088 x 1088	608 x 608	82.6	91.4	1.6
YOLOV4-tiny@608	4032 x 3024	1088 x 1088	1088 x 1088	77.9	83.4	1
YOLOV4-tiny@608	4032 x 3024	1088 x 1088	832 x 832	85.9	92.7	1.3
YOLOV4-tiny@608	4032 x 3024	1088 x 1088	608 x 608	81.9	89.3	1.7
YOLOV4-tiny@416	4032 x 3024	832 x 832	1088 x 1088	53.3	57.6	1
YOLOV4-tiny@416	4032 x 3024	832 x 832	832 x 832	66	71.9	1.1
YOLOV4-tiny@416	4032 x 3024	832 x 832	608 x 608	81.4	88.1	1.6
YOLOV4-tiny@512	4032 x 3024	832 x 832	1088 x 1088	66.7	72.8	1
YOLOV4-tiny@512	4032 x 3024	832 x 832	832 x 832	79.1	85.0	1.1
Without tiling						
YoloV4-tiny@416	4032 x 3024	-	-	54	21	0.15
YoloV4-tiny@512	4032 x 3024	-	-	69	48	0.15
YoloV4-tiny@608	4032 x 3024	-	-	76	57	0.15

Bold values indicate the best-performing model of 95.1% and most common precision of 87.4%. The giant measurement mannequin (YOLOV4-MOD) with enter decision of 416 x 416 executed a most recall of 95.1% and most common precision of 85.5% with the aid of the usage of a coaching tile dimension of 1088 x 1088 and inference tile measurement of 832 x 832. YOLOV4-tiny and YOLOV4-tiny-3l function 2.6x and 2x quicker in contrast to YOLOV4MOD with higher recall and common precision respectively. Surprisingly, light-weight models obtain a higher trade-off between detection overall performance and inference velocity for P. falciparum detection in contrast to the giant YOLOV4-MOD mannequin by using leveraging the proposed tile-based approach. Among the light-weight models, YOLOV4-tiny was once chosen as the first-rate mannequin with similar overall performance with YOLOV4-tiny-3l however has excessive computation speed. Comparison to Baseline method: The proposed detection models' overall performance was once additionally in contrast with the baseline approach which at once applies high resolution snap shots throughout mannequin coaching and inference. As proven in Table 2 overall performance of fashions the usage of the proposed tile-based strategy indicates large overall performance enhancement in contrast to their baseline counterparts.

Compared to their baseline models, light-weight fashions operate 10× slower in computation pace however their detection overall performance amplify with a big amount, which is about 17% in phrases of recall for yolov4-tiny-3l and about 38% for the yolov4-tiny model Assessment of the chosen mannequin on exterior datasets: Furthermore, overall performance of the chosen mannequin (YOLOV4-tiny) used to be evaluated on two exterior datasets accrued from a unique domain. By using the first exterior dataset which is a low-resolution photograph received from [10], an common precision of 57.8% and recall of 75.1% used to be executed by way of the use of the complete dataset as take a look at data. Similarly, with the aid of the usage of the 2d exterior statistics acquired from [28] an common precision of 71.1% and recall of 86.3% used to be achieved.

In addition, the chosen mannequin used to be fine-tuned and evaluated by means of partitioning the two exterior datasets into training, validation, and trying out and merging them with the mannequin improvement dataset. In that way, an common precision of 83.4% and a recall of 94.7% was once performed on check statistics of the first exterior dataset and an common precision of 73.1% and recall of 96.3% was once completed on check records of the 2nd exterior dataset. After selection of the best model among the three proposed detection models, its P. falciparum detection performance was tested on the first and second external datasets described in section. When the selected model was evaluated using the first external dataset tile-based processing was not applied since resolution of the dataset is not high compared to the proposed detection network's input resolution. The second external dataset consists of high-resolution thick smear microscopic images and the tile-based approach was applied when it was evaluated using this dataset. Furthermore, two experimental setups were followed during evaluation of the selected model using these two external datasets. In the first experimental setting, the selected model was evaluated by utilizing the whole dataset as test data. In the second experimental setting, the datasets were partitioned into training, validation and combined with the model development dataset to fine-tune the selected model. In addition, the selected model was evaluated on 1141 uninfected images collected from 50 uninfected patients which have not been used during model training.

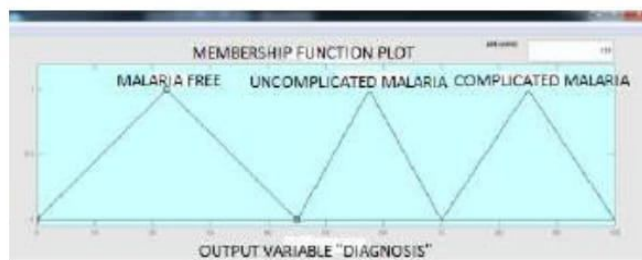


Figure 4: Output variable

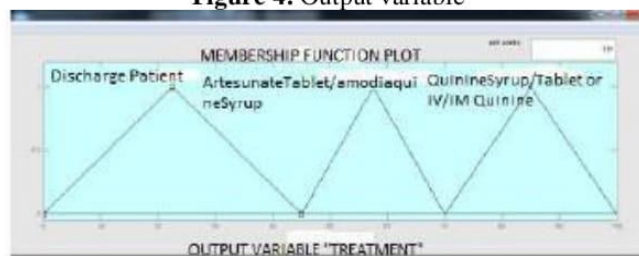


Figure 5: Output: Treatment

This dataset is a high-resolution thick smear microscopic image and has a resolution of 4032 x 3024 pixels. Thus, the proposed tile-based approach was applied to investigate performance of the selected model on identifying uninfected images. Deep learning-based fashions for herbal object detecfashions operate poorly on small object detection dutiestion exhibit promising results, their software for a such as malaria parasite detection. The different project unique area such as malaria parasite screening has is associated to high-resolution microscopic pixbenits personal challenges. Existing SOTA object detectionefited from the development in digital statistics acquisition applied sciences such as high-resolution cameras. Directly making use of high-resolution pix by using downscaling to SOTA detection network's low decision enter degrades small object detection overall performance due to the element data

CONCLUSION

Besides, the proposed fashions have been evaluated the usage of datasets bought from a unique area to validate their generalization capacity and detection accuracy. Based on the good sized experimental analysis, light-weight YOLOV4 based totally fashions done a considerable overall performance enhancement the use of the proposed tile-based method with 38% overall performance raise regarding their baseline method, whilst requiring solely minimal extra computation cost. In addition, the proposed technique outperforms detection outcomes bought by way of preceding lookup works the usage of comparable datasets. The proposed malaria parasite screening approach has the plausible to minimize workload of laboratory technicians by using presenting actual parasite places or suspicious areas so that it will help the docs to make their remaining choice.

REFERENCES

1. WHO. World malaria report 2021. Geneva: World Health Organization; 2021. Licence: CC BY-NC-SA 3.0
2. Samuel Shillcutt, Chantal Morel, Catherine Goodman, Paul Coleman, David Bell, Christopher Whitty, and Anne Mills. Cost-effectiveness of malaria diagnostic methods in sub-saharan africa in an era of combination therapy. *Bulletin of the World Health Organization*, 86: 101–10, 03 2008. .
3. Mahdieh Poostchi, Kamolrat Silamut, Richard Maude, Stefan Jaeger, and George Thoma. Image analysis and machine learning for detecting malaria. *Translational Research*, 194, 01 2018. .
4. Karan Makhija, Samuel Maloney, and Robert E Norton. The utility of serial blood film testing for the diagnosis of malaria. *Pathology*, 47: 68–70, 2015.
5. Kassahun Desta, G. Mengistu, and Beteley Gelaw. The reliability of blood film examination for malaria at the peripheral health unit. *Ethiopian J Health Dev*, 17, 01 2004.
6. Fatima A. Merchant and Kenneth R. Castleman. Chapter 27 computer-assisted microscopy. In AI Bovik, editor, *The Essential Guide to Image Processing*, pages 777–831. Academic Press, Boston, 2009. ISBN 978-0-12-374457-
7. Feng Yang, Mahdieh Poostchi, Hang Yu, Zhou Zhou, Kamolrat Silamut, Jian Yu, Richard James Maude, Stefan Jaeger, and S. Antani. Deep learning for smartphone-based malaria parasite detection in thick blood smears. *IEEE Journal of Biomedical and Health Informatics*, 24: 1427–1438, 2020.
8. A. Gokul, Anna University Regional Campus Madurai; E. Shanmuga priya, Anna university Regional Campus Madurai. "Energy Optimization in Cloud Computing by EGC Algorithm." *Global Research and Development Journal For Engineering*: 10 - 12.
9. Manikandan.S, S.Suganthi and Gayathiri. R, "Optimal Energy Efficiency Techniques and Security Enhancement in Wireless Sensor Network Using Machine Learning," 2022 International Conference on Power, Energy, Control and Transmission Systems (ICPECTS), Chennai, India, 2022, pp. 1-5, <https://doi.org/10.1109/ICPECTS56089.2022.10046790>.